

## **Electronic Supplementary Information accompanying “Structurally and Electronically Driven Uniaxial Negative Thermal Expansion in BaIrO<sub>3</sub>”**

Alexander J. Browne,<sup>a,b</sup> Andrew D. Fortes,<sup>c</sup> Andreas W. Rost<sup>b\*</sup> and Alexandra S. Gibbs,<sup>a,c</sup>

<sup>a</sup> School of Chemistry, University of St Andrews, St Andrews, KY16 9ST, UK.

<sup>b</sup> School of Physics and Astronomy, University of St Andrews, St Andrews, KY16 9SS, UK.

<sup>c</sup> ISIS Pulsed Neutron and Muon Source, STFC Rutherford Appleton Lab, Harwell Campus, Didcot, OX11 0QX, UK.

Email: a.rost@st-andrews.ac.uk

### Methods:

4.5g of BaIrO<sub>3</sub> was synthesised by a solid-state reaction. Powders of BaCO<sub>3</sub> (Sigma-Aldrich, 99%; pre-dried at 650°C overnight) and <sup>193</sup>Ir (Isoflex 99.46 atom% enriched) in the stoichiometric ratio were ground together in an agate pestle and mortar then pressed into a pellet, which was heated in a covered alumina crucible. A total of seven heating steps (1000°C for 12h; 1000°C for 48h; 1050°C for 48h; 1100°C for 36h; 1150°C for 48 h; 1150°C for 18h; 1200°C for 60h) were required, with the pellet ground and re-pressed between each. Enriched <sup>193</sup>Ir was used to minimise neutron absorption.<sup>1</sup>

Powder neutron diffraction data were collected using the HRPD beamline,<sup>2</sup> ISIS Pulsed Neutron and Muon Source (data DOI [10.5286/ISIS.E.RB1910632](https://doi.org/10.5286/ISIS.E.RB1910632)). The sample was held in an aluminium slab can with vanadium windows. A closed cycle refrigerator was used for cooling.

Rietveld refinements were done using TOPAS Academic, V7.<sup>3</sup> Crystal structure diagrams were prepared using VESTA3.<sup>4</sup> Symmetry-mode analysis was done using ISODISTORT.<sup>5</sup>

The magnetic susceptibility was obtained using a Quantum Design MPMS3, measuring in an applied field of 0.1 T.

### Fits to the principal lattice strains $\epsilon_{X_i}$ :

As discussed in the main text, lattice strains  $\epsilon_{X_i}$  along the orthogonal principal axes  $X_i$  were obtained using PASCAL.<sup>6</sup> These data are plotted in Fig. 1b (using a percentage scale) and again in Fig. S1 (using an absolute scale). Using an absolute scale allows fits to determine the linear thermal expansion coefficients  $\alpha_{X_i}$  to be made. At high temperatures, the linear relationship  $\epsilon_{X_i} \propto \alpha_{X_i} T$  is valid. To account for the slight change in gradient that occurs on crossing  $T_C = 184$  K, two linear fits were made to each  $\epsilon_{X_i}$ : one between 80 K and 182 K, and one between 186 K and 270 K. Data for 280-300 K

were excluded due to a discontinuity (most visible in  $\epsilon_{X1}$ ) which we believe to be an experimental artifact and not intrinsic behaviour. At very low temperatures this linear behaviour breaks down; between 10 and 60 K, all three  $\epsilon_{Xi}$  could be fit with  $\epsilon_{Xi} \propto T^3$ , as per the Debye model.

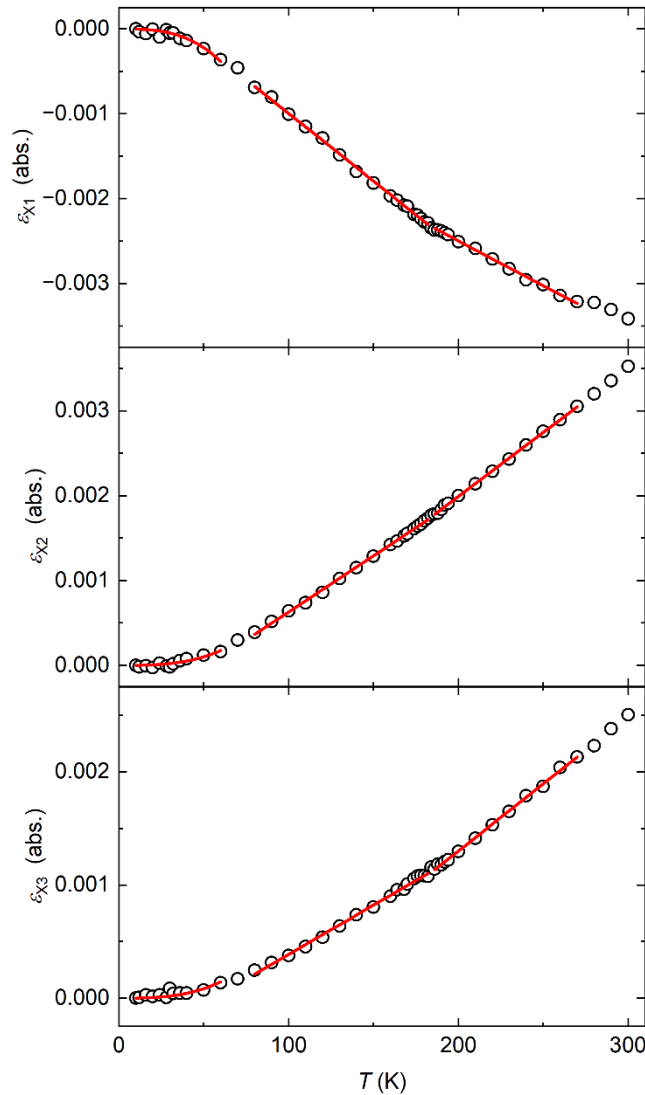


**Fig. S1 Fits to the lattice strains  $\epsilon_{Xi}$ .**

Determining the volumetric thermal expansion coefficient  $\alpha_V$ :

The volumetric thermal expansion coefficient can be defined<sup>7</sup> as

$$\alpha_V = \frac{1}{V_0} \times \frac{dV}{dT}$$

We show the variation of volume with temperature in Fig. 1b; an expansion of the low-temperature regime is shown in Fig. S2. Whilst  $V$  starts to increase when  $T > 100$  K, it is effectively constant at lower temperatures. A linear fit between 10 K and 100 K gives  $dV/dT = 1.6(2.0) \times 10^{-4} \text{ \AA}^3 \text{ K}^{-1}$  and  $V_0 = 848.43(1) \text{ \AA}^3$ , and together these determine the average  $\alpha_V = 1.9(2.0) \times 10^{-7} \text{ K}^{-1}$  in this temperature range.

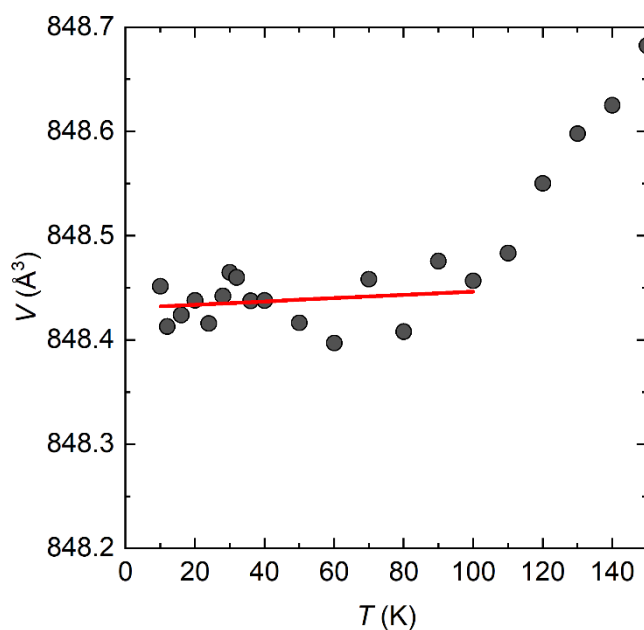


**Fig. S2** The unit cell volume as a function of temperature, with a linear fit between 10 K and 100 K.

---

<sup>1</sup> A. C. Hannon, A. S. Gibbs and H. Takagi, *J. Appl. Cryst.*, 2018, **51**, 854-866.

<sup>2</sup> A. D. Fortes and A. S. Gibbs, *J. Neutron Res.*, 2020, **22**, 91-98.

<sup>3</sup> A. A. Coelho, *J. Appl. Cryst.*, 2018, **51**, 210-218.

<sup>4</sup> K. Momma and F. Izumi, *J. Appl. Cryst.*, 2011, **44**, 1272-1276.

<sup>5</sup> (a) H. T. Stokes, D. M. Hatch, and B. J. Campbell, ISODISTORT, ISOTROPY Software Suite, iso.byu.edu. (b) B. J. Campbell, H. T. Stokes, D. E. Tanner, and D. M. Hatch, *J. Appl. Cryst.*, 2016, **39**, 607-614.

<sup>6</sup> M. Lertkiatrakul, M. L. Evans, and M. J. Cliffe, *J. Open Source Softw.*, 2023, **8**, 5556.

<sup>7</sup> J. Chen, L. Hu, J. Deng and X. Xing, *Chem. Soc. Rev.*, 2015, **44**, 3522-3567.